DEVELOPMENT OF A GROUND-BASED TOMOGRAPHIC SAR SYSTEM

Younghun Ji, Hyangsun Han and Hoonyol Lee*

Department of Geophysics, Kangwon National University, Republic of Korea
*Corresponding author: hoonyol@kangwon.ac.kr

ABSTRACT: Synthetic Aperture Radar (SAR) provides high-resolution images regardless of weather conditions and solar illumination. However, a SAR image projects the 3D distributed targets onto a 2D plane in range and azimuth. Tomographic SAR (TomoSAR) is a technique to generate 3D image by adding the vertical baselines to the conventional SAR image acquisition. TomoSAR has recently been used to map the internal structure of forests and the geometry of the buildings by using airborne and ground-based SAR systems. In this paper, we report the construction of a Ground-Based TomoSAR (GB-TomoSAR) system and explain the basic principle of the GB-TomoSAR focusing algorithm. A GB-TomoSAR experiment was performed on the rooftop of a building at Kangwon National University. We also describe the principle of geometric and radiometric corrections in order to enhance the quality of the images. Heights of various targets were measured by generating the slice images both in the horizontal and vertical direction, which well matched to the *in situ* data. The experimental image has limitations in the detection of trees due to temporal decorrelation during the 8 hours of acquisition for a single tomogram. In order to overcome this limitation, we are planning to enhance the scanning speed of GB-TomoSAR in the near future.

KEY WORDS: Tomographic SAR, 3D focusing algorithm, Geometric correction, 3D SAR simulation, Radiometric correction

1. INTRODUCTION

Synthetic Aperture Radar (SAR) provides high resolution images regardless of weather conditions and sun altitudes. SAR has been widely used for various scientific fields and military purposes. However, SAR image represents the 3-dimensionally (3D) distributed targets onto a 2-dimensional (2D) plane in the range and azimuth directions. Tomographic SAR (TomoSAR) is a technique to generate 3D image by obtaining SAR images with various vertical baselines (Zhu and Bamler, 2010). TomoSAR has been used to map the internal structure of forests and the layover of the buildings (Lopez-Sanchez and Fortuny-Guasch, 2000; Xing *et al.,* 2013).

In this study, we develop a GB-TomoSAR system based on a Ground-Based SAR (GB-SAR) and explain the basic principles of the 3D focusing algorithm and radiometric and geometric correction. We tested the 3D focusing algorithm by simulation. The heights of various targets are measured by generating the slice images in the range-azimuth and range-vertical planes. We verify the performance of the GB-TomoSAR system and the 3D focusing algorithm by comparing the heights of the targets measured by GB-TomoSAR with those by *in situ* survey.

2. 3D SAR FOCUSING ALGORITHM

Principle of the tomographic SAR focusing is analogous to the GB-SAR. GB-SAR generate a 2D image by moving the antenna along the azimuth. GB-TomoSAR repeats the acquisition of GB-SAR data by moving the rail system stepwise in vertical direction. Focusing algorithm of range-vertical plane is similar to a rotated focusing algorithm in the range-azimuth plane. In this study, we get the 3D SAR image by extending a one-dimensional deramp-FFT algorithm in azimuth direction for GB-SAR focusing to two-dimensional deramp-FFT in azimuth and vertical direction. Fig. 1 shows the block diagram of the 2D deramp-FFT algorithm for GB-TomoSAR focusing.

2.1 Range compression

The received signal of GB-TomoSAR is obtained in the stepped-frequency format in frequency domain by a vector network analyzer.

$$S(f) = H(f)G(f) \tag{1}$$

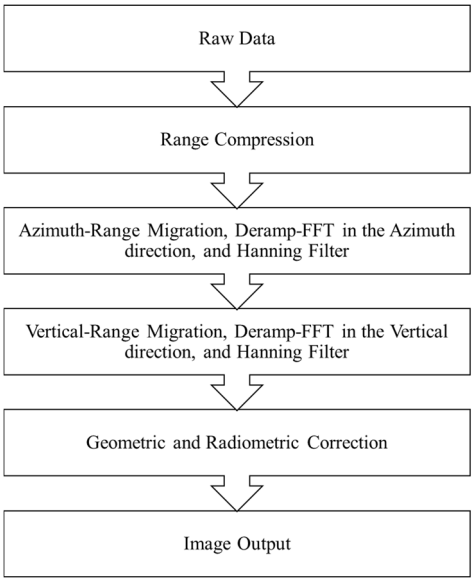

Fig. 1. Block diagram of 2D deramp-FFT algorithm.

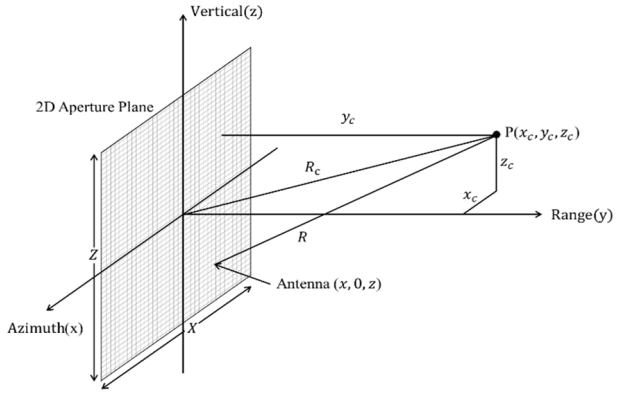

Fig. 2. Measurement and imaging geometry.

where $H(f)$ is the box function with a center at f_c and a bandwidth of B_R. It shows the frequency field of the transmitted and received microwave. $G(f)$ is the reflection coefficient of the target as a function of frequency. Equation (1) can be changed to the time domain by using inverse Fourier transform, which can be expressed by using convolution as

$$s(t) = h(t) * g(t). \tag{2}$$

If the target is placed at a two-way travel time of $t = t_0 = 2R/c$, and the reflection coefficient of the target is $g(t) = \delta(t - t_0)$, then the equation (2) can be expressed as follows:

$$s(t) = B_R \text{sinc}[\pi B_R(t - t_0)]\exp[j2\pi f_c(t - t_0)] \tag{3}$$

Maximum of $s(t)$ has at $t = 2R/c$, and the phase term is the distance of target from the sensor. Time resolution is given as $\delta t = 1/B_R$, and range resolution is calculated by $\delta R = c\delta t/2 = c/2B_R$ (Lee *et al.*, 2007).

2.2 2-Dimensional Deramp-FFT Algorithm

Deramp-FFT algorithm is performed by multiplying the deramp function to the range compressed signal and then applying the inverse Fourier transform. This algorithm regards that the obtained signal is in frequency domain due to the time-frequency locking phenomenon of a SAR system. It uses lower memory and less processing time than other focusing algorithms such as range-Doppler algorithm. Therefore it can be useful for near-real time SAR focusing.

If a target is located at P(x_c, y_c, z_c), as shown in Fig. 2, the range-compressed signal received a various antenna location at $(x, 0, z)$ is expressed as follows:

$$s(x, z|x_c, y_c, z_c) = e^{-j\frac{4\pi}{\lambda}R(x,z|x_c,y_c,z_c)} \tag{4}$$
$$|x - x_c| < y_c\frac{\lambda}{L_x} and |x| \le X/2$$
$$|z - z_c| < y_c\frac{\lambda}{L_z} and |z| \le Z/2$$

where λ = wavelength
x, z = antenna location in baseline
X, Z = aperture length of azimuth and vertical
L_x, L_z = antenna aperture size of row and column

R is the range to the target, i. e.,

$$R(x, z) = \sqrt{(x - x_c)^2 + y_c^2 + (z - z_c)^2} \tag{5}$$

We apply the 2D Taylor series to equation (5) at the center of antenna scan field at $(x, z) = (0, 0)$.

$$R(x, z|x_c, y_c, z_c) = R(0,0) + (R_x(0,0)x + R_z(0,0)z) + \frac{1}{2}(R_{xx}(0,0)x^2 + 2R_{xz}(0,0)xz + R_{zz}(0,0)z^2) + \cdots \tag{6}$$

Equation (4) and (6) can be merged to

$$s(x, z|x_c, y_c, z_c) = e^{-j\frac{4\pi}{\lambda}(R_c - \left(\frac{x_c}{R_c}x + \frac{z_c}{R_c}z\right) + \left(\frac{y_c^2 + z_c^2}{2R_c^3}x^2 - \frac{x_c z_c}{R_c^3}xz + \frac{y_c^2 + x_c^2}{2R_c^3}z^2\right) + \cdots)} \tag{7}$$

During the data processing, we arrange the received signal by using the range migration, multiply the 2D deramp function ($h^{-1}(x, z)$), apply the Hanning filter, and then use the 2D iFFT (Fig. 1).

$$h^{-1}(x, z) = e^{j\frac{4\pi}{\lambda}(\frac{y_c^2 + z_c^2}{2R_c^3}x^2 - \frac{x_c z_c}{R_c^3}xz + \frac{y_c^2 + x_c^2}{2R_c^3}z^2)} \tag{8}$$

$$g(u, v) = \int_{-\infty}^{\infty}\int_{-\infty}^{\infty} s(x, z)h^{-1}(x, z)e^{-j2\pi ux}e^{-j2\pi vz}dxdz \tag{9}$$

Equation (9) can be calculated analytically as follows:

$$g(u, v) = e^{-j\frac{4\pi}{\lambda}R_c}XZ\text{sinc}[X\pi(u - \frac{2x_c}{\lambda R_c})]\text{sinc}[Z\pi(v - \frac{2z_c}{\lambda R_c})] \tag{10}$$

Maximum of $g(u, v)$ occurs at $u = 2x_c/\lambda R_c$, $v = 2z_c/\lambda R_c$. Geocoding should be followed according to those equations. Resolutions are given as $\delta u = 1/X$, $\delta v = 1/Z$, which can be expressed as the azimuth and vertical resolution ($\delta x_c, \delta z_c$) as follows:

$$\delta x_c = \frac{\lambda R_c}{2X}, \delta z_c = \frac{\lambda R_c}{2Z}. \tag{11}$$

2.3 Radiometric Correction

We applied the radiometric correction to the 3D image by using antenna radiation pattern. Radiometric correction is based on radar equation as follows (Stutzman and Thiele, 1998):

$$P_r = P_t\frac{\lambda^2 G^2}{(4\pi)^3 R^4}\sigma \tag{12}$$

where P_r = received power
P_t = transmitted power
G = antenna gain pattern
R = range
σ = radar cross section

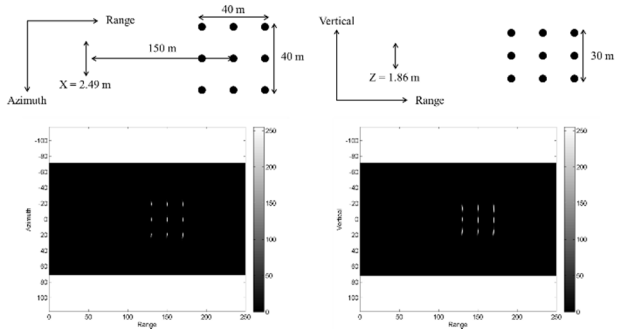

Fig. 3. Distribution of point scatters used in the TomoSAR simulation, and slice images of the 3D SAR simulation data after focusing.

Radiometric correction term (RC) can be calculated by dividing P_0, the received power of a target at a reference point, by P_r, the power of a target as

$$RC = \frac{P_0}{P_r} = \frac{(R/R_0)^4}{(G/G_0)^2} \qquad (13)$$

The dB of equation (13) is added to the geocoded 3D TomoSAR image.

3. SIMULATION OF GB-TOMOSAR DATA

We simulate the GB-TomoSAR system to verify the developed focusing algorithm. The computer codes of the algorithm has been implemented in the MATLAB. The target consists of a 3D array of $3 \times 3 \times 3$ point scatters as shown in Fig. 3. The system specification of the simulation is shown in Table 1, which is identical to those of the field experiment in the next section. We also added random noise to the raw signal.

Fig. 3 shows the simulation result showing range-azimuth and range-vertical slice image in the image center line. The image clearly shows the focused point targets at the original location. Therefore, we confirmed that the 2D deramp-FFT algorithm is correct and useful for the 3D TomoSAR imaging.

Table 1. Specification of GB-TomoSAR system for the simulation and the experiment

Symbol	Quantity	Values
f_c	Radar Center Frequency	5.3 GHz
B_R	Radar Bandwidth	600 MHz
Δf	Frequency Step	0.3 MHz
X	Azimuth Scan Length	2.49 m
Z	Vertical Scan Length	1.86 m
Δx	Azimuth Scan Step	0.03 m
Δz	Vertical Scan Step	0.03 m
/	Radar Polarization	VV
a	Antenna Beam Width	15 °
H_b	Initial Antenna Height	18 m

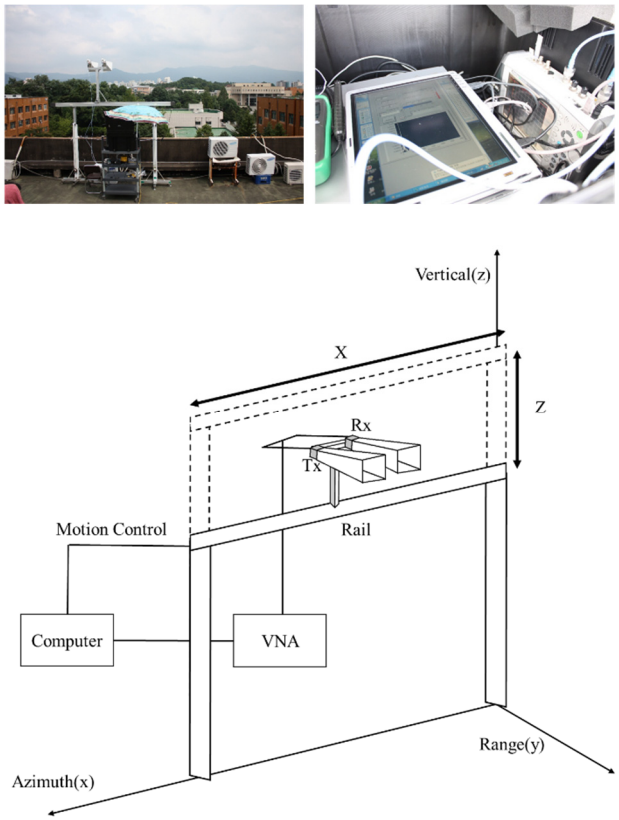

Fig. 4. Pictures and diagram of GB-TomoSAR system.

4. EXPERIMENT AND RESULTS

The picture and a diagram of the GB-TomoSAR system is shown in Fig. 4. The azimuth resolution is achieved by moving the antenna along the horizontal rail of the GB-SAR while the vertical resolution was made by changing the height of the horizontal rail. A vector network analyser (Anritsu Master MS2028B) generated microwave signal and measured the returned scattering. A 30W power amplifier was attached before the transmission antenna. The notebook computer controlled the motion of antenna, initiate the acquisition and collected the data. According to the specification of GB-TomoSAR system given in Table. 1, the range resolution δR, the azimuth angular resolution $\delta\theta$ and the vertical angular resolution $\delta\varphi$ is calculated to be 0.244 m, 0.675 °, and 0.871 °, respectively. Fig. 5(a) shows the scan area of the TomoSAR experiment and Fig. 5(b) illustrates 3D conceptual diagram of TomoSAR data. GB-TomoSAR experiment was performed on the rooftop of Science College at Kangwon National University during 8 hours. Main targets are university buildings, roads and trees of 20 ~ 30 m height that triggers large volume scattering.

Fig. 6(a) and (b) shows the range-azimuth slice image that includes the image center line and that on the plane slanted by 7.84 ° downwards from the image center line, respectively. All images were shown after the geometric and radiometric corrections. The library building and building B are clearly shown in Fig. 6(a) but not detected in Fig. 6(b) which imaged below horizon in this range. From the distinctive features between Fig. 6(a) and (b), we could verify that the GB-TomoSAR system based on GB-

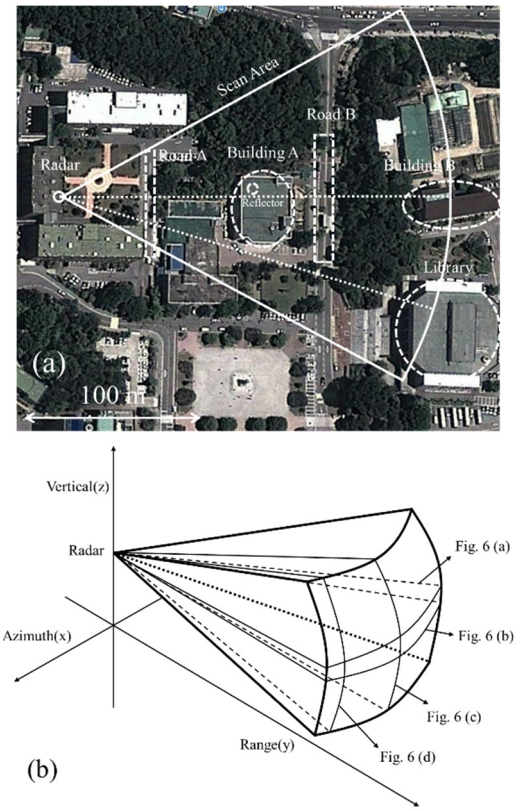

Fig. 5. Scan area of the GB-TomoSAR experiment (a) and 3D conceptual diagram of GB-TomoSAR data (b).

SAR was constructed and focused successfully. The two dotted lines in Fig. 6(a) represent the vertical slice lines to obtain the range-vertical slice images shown in Fig. 6(c) and (d) separated by an angle of 24.2 °.

The dotted lines in Fig. 6(c) represent the border of buildings and roads in the vertical direction. We could distinguish the various structures located along the two vertical slice lines. The heights of the library and building B were measured to be 30±3 m from Fig. 6(c) and (d), which were well matched to the *in situ* heights of the library (30 m) and building B (23 m). However, the tomographic image has a limitation of the detection of tress due to the temporal decorrelation of the trees during the 8 hours of GB-TomoSAR experiment.

5. CONCLUSION

We developed a GB-TomoSAR system based on GB-SAR to generate the 3D tomographic image of targets. A 3D SAR focusing algorithm was successfully developed by extending a one-dimensional deramp-FFT algorithm used for GB-SAR focusing to 2D azimuth-vertical field. Simulation of TomoSAR verified the TomoSAR algorithm, focusing software, and geometric and radiometric calibrations. GB-TomoSAR system provided reasonable heights of stable buildings and roads. However, trees were poorly detected due to the temporal decorrelation caused by the wind during the experiment. We have a plan to enhance the scanning speed of the GB-TomoSAR system to reduce the temporal effects of an unstable targets.

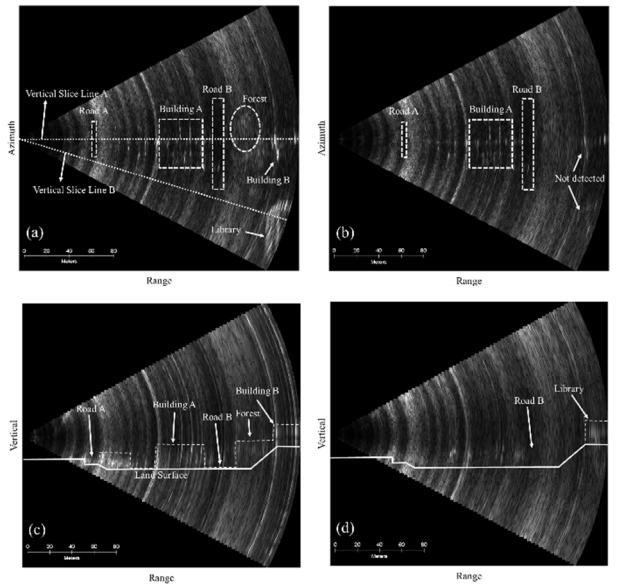

Fig. 6. Slice images of 3D GB-TomoSAR. Range-azimuth slice image including the image center line (a) and that on a plane slanted by 7.84 ° downwards from the image center line. Range-vertical slice image along the slice line A (c) and B (d).

ACKNOWLEDGEMENTS

This research was supported by Space Core Technology Development Program through the NRF funded by the Ministry of Science, ICT and Future Planning (NRF-2013M1A3A3A02041853) and also by Basic Science Research Program through the National Research Foundation of Korea (NRF) funded by the Ministry of Education (NRF-2013R1A1A2008062).

REFERNCES

Lee, H., S. J. Cho, N. H. Sung, and J. H. Kim, 2007. Development of a GB-SAR (Ⅱ) : focusing algorithms. *Korean Journal of Remote Sensing*, 23(4), pp. 247-256.

Lopez-Sanchez, J. M., and J. Fortuny-Guasch, 2000. 3-D radar imaging using range migration techniques. *IEEE Transactions on Antennas and Propagation,* 48(5), pp. 728-737.

Stutzman, W. L., and G. A. Thiele, 1998. *Antenna Theory and Design 2nd edition*. John Wiley & Sons, New York, pp. 486-487.

Xing, S., Y. Li, D. Dai, and X. Wang, 2013. Three-dimensional reconstruction of man-made objects using polarimetric tomographic SAR. *IEEE Transactions on Geoscience Remote Sensing*, 51(6), pp. 3694-3705.

Zhu, X. X., and R. Bamler, 2010. Tomographic SAR inversion by L_1 -norm regularization-the compressive sensing approach. *IEEE Transactions on Geoscience Remote Sensing*, 48(10), pp. 3839-3846.